PROCEEDINGS OF SPIE

SPIEDigitalLibrary.org/conference-proceedings-of-spie

Wavefront sensing for active alignment control of a telescope with dynamically varying pupil geometry: theory, implementation, on-sky performance

Lee, Hanshin, Hill, Gary, Drory, Niv, Ramsey, Jason, Bryant, Randy, et al.

Hanshin Lee, Gary J. Hill, Niv Drory, Jason Ramsey, Randy Bryant, Matthew Shetrone, "Wavefront sensing for active alignment control of a telescope with dynamically varying pupil geometry: theory, implementation, on-sky performance," Proc. SPIE 10706, Advances in Optical and Mechanical Technologies for Telescopes and Instrumentation III, 107064P (10 July 2018); doi: 10.1117/12.2314101

SPIE.

Event: SPIE Astronomical Telescopes + Instrumentation, 2018, Austin, Texas, United States

Wavefront sensing for active alignment control of a telescope with dynamically varying pupil geometry: Theory, Implementation, On-sky Performance

Hanshin Lee[a], Gary J. Hill[a], Niv Drory[a], Jason Ramsey[a], Randy Bryant[b], Matthew Shetrone[b]
[a]McDonald Observatory, University of Texas at Austin, 2515 Speedway, C1402, Austin, TX, USA 78712-0259;
[b] Hobby-Eberly Telescope, University of Texas at Austin

ABSTRACT

Unlike conventional astronomical telescopes, there are telescope systems that have fixed altitude primary mirrors over which prime focus cameras track the sidereal motion. Examples include the Hobby Eberly Telescope (HET) in Texas and the South African Large Telescope (SALT) in Cape Town. These systems benefit from the economy of fixed primary mirrors but pose a unique challenge in active alignment control of such telescope systems using wavefront sensor feedbacks. To handle this situation, we developed a way of estimating orthonormal aberration coefficients over dynamically varying pupil geometries and implemented this as part of the multi-year upgrade of the HET. We detail the theory, implementation, and on-sky performance of this technique in the active alignment control of the HET based on the data collected during the HET upgrade commissioning and science operations since late 2015.

Keywords: Wavefront Sensing, Non-circular pupil, Dynamically varying pupil, Active alignment control, Hobby-Eberly Telescope

1. INTRODUCTION

Almost all astronomical telescopes are constructed in such a way that the whole telescope structure as well as the optical axis tracks the sidereal motion. These telescopes also have their aperture stop near or at their primary mirrors. As a result, their pupil geometries (mostly annular) are stationary independent of pointing. There are also telescope systems that feature a fixed altitude primary mirror with a prime focus camera tracking over the primary mirror to follow the sidereal motion. Such telescope systems tend to have fixed aperture stop somewhere inside the prime focus camera and its projection onto the primary mirror constantly moves during a track. For largely economic reasons, the primary mirrors of such telescopes are not large enough to completely enclose the project pupil across two extreme track positions. As a result, the telescope's effective pupil constantly changes in shape over a track and this poses a unique challenge in active alignment control of such telescope systems using wavefront sensor feedbacks. Examples include the Hobby Eberly Telescope (HET) in Texas and the South African Large Telescope (SALT) in Cape Town. In an effort to handle this unique situation, we, at the HET, have developed a way of estimating orthonormal aberration coefficients on dynamically varying pupil geometries. The method is based on the fact that all necessary pieces of information for constructing orthonormal polynomials (via the Gram–Schmidt process) can be numerically obtained during a routine least-squares fit of Zernike polynomials to wavefront data. This allows the method to use the usual Zernike polynomial fitting with an additional procedure that swiftly estimates the desired orthonormal aberration coefficients without having to use the functional forms of orthonormal polynomials and numerical integration process. With these features, we anticipated that the method could be ideal for real-time wavefront analysis on telescopes like HET, which is otherwise inefficient with analytic methods used in past studies. This wavefront analysis technique has been implemented in our multi-year upgrade of the HET that has just been completed. In this paper, we detail the theory, implementation, and on-sky performance of this technique in the active alignment control of

Advances in Optical and Mechanical Technologies for Telescopes and Instrumentation III, edited by Ramón Navarro, Roland Geyl, Proc. of SPIE Vol. 10706, 107064P · © 2018 SPIE
CCC code: 0277-786X/18/$18 · doi: 10.1117/12.2314101

the HET based on the data collected during the HET upgrade commissioning and science operations since late 2015.

2. CONTEXT

The HET will be upgraded with a 22-arcmin. diameter field of view wide field corrector (WFC), a new tracker and prime focus instrument package (PFIP), and new metrology systems [1]. The new corrector has much improved image quality and a 10 m pupil diameter. The periphery of the field will be used for guiding and wavefront sensing to provide the necessary feedback to keep the telescope correctly aligned. The WFC will give 30 times larger observing area than the current HET corrector. It is a four-mirror design with two concave 1 meter diameter mirrors, one concave 0.9 meter diameter mirror, and one convex 0.23 m diameter mirror. The corrector is designed for feeding optical fibers at f/3.65 to minimize focal ratio degradation, and so the chief ray from all field angles is normal to the focal surface. This is achieved with a concave spherical focal surface centered on the exit pupil. The primary mirror spherical aberration and the off-axis aberrations in the wide field are controllable due to the first two mirrors being near pupils, and the second two mirrors being well separated from pupils. The imaging performance is 0.5 arcseconds or better over the entire 22 arcminute field of view, and vignetting is minimal.

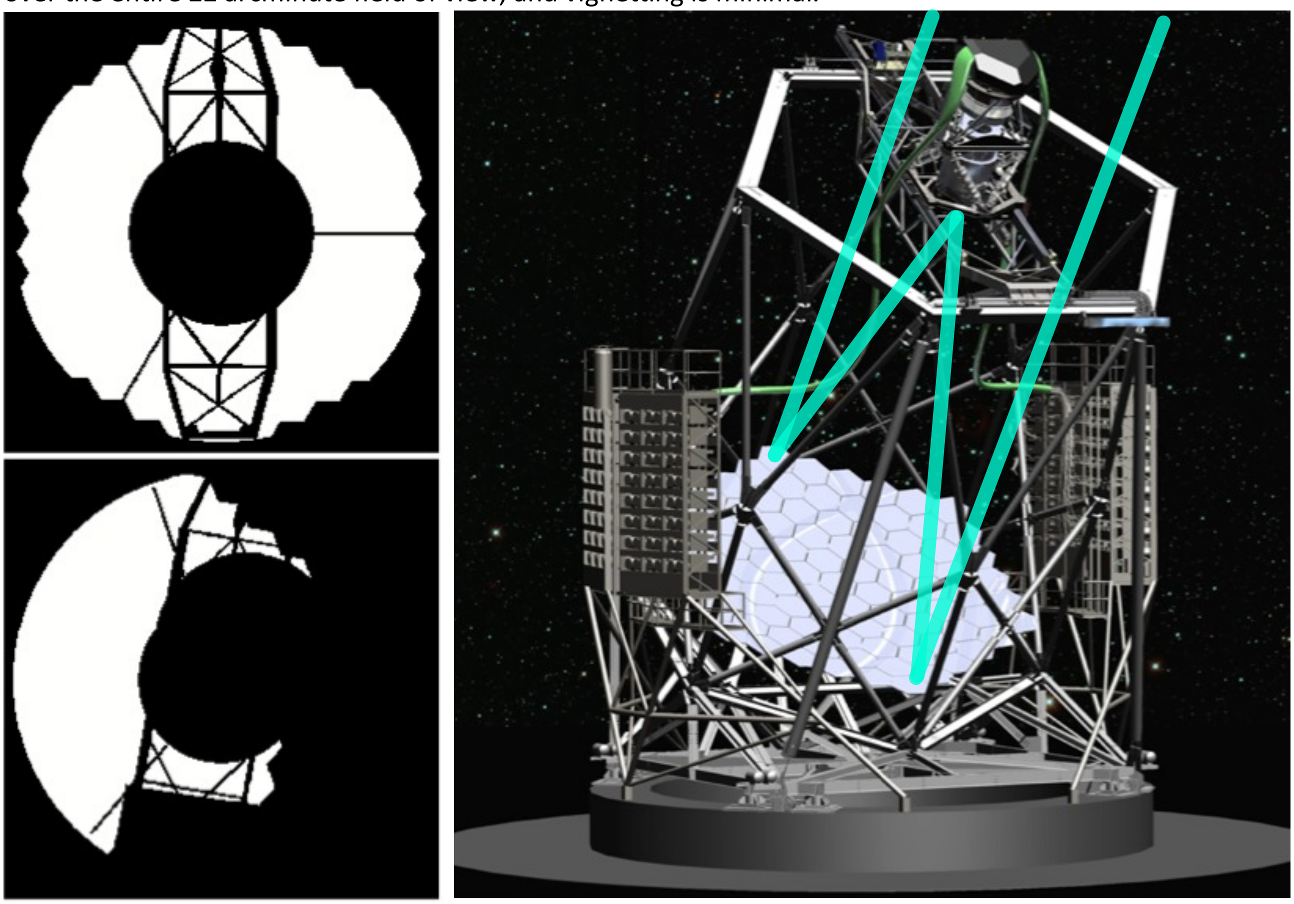

Figure 1 (Left) Example images from the HET pupil models at various tracker positions and field locations. (Right) the HET with its fixed primary and tracker system.

Wavefront sensing (WFS) is one of the key elements for active alignment of the WFC, as it tracks sidereal motion, with respect to the fixed HET primary mirror[2,3]. During a track, part of the 10m-pupil of the WFC can lie outside the primary periphery and be clipped off. An additional field-dependent central obscuration by the holes and baffles of the WFC leads to complex pupil geometries. The combination of these is a complicated dynamically varying non-circular telescope pupil. This unique problem to the WFS on the HET needs to be dealt with by choosing an appropriate set of orthonormal aberration polynomials during wavefront reconstruction. Zernike polynomials, that constitute one particular orthonormal set over a unit disk, have been applied to various fields [2–4]. However, there are increasingly many optical systems whose pupils are non-circular. In addition, some systems exhibit variability in pupil shape as a function of field and/or pointing angles as the HET. On such pupils, Zernike polynomials loose orthogonality and it is desirable to use the coefficients of new orthonormal aberration polynomials.

Studies show that orthonormal polynomials can be analytically constructed, via the Gram-Schmidt process, for non-circular pupils in simple shape without shape variability, i.e. annulus, hexagon, ellipse and rectangle [7–10]. The studies overlook implementation aspect of the analytic method to wavefront data measured over more complex pixelated pupil shapes (due to pixel-based imaging sensors) with dynamic variability where the ability to obtain orthonormal aberration coefficients can be highly advantageous. Thus, potential issues in using the method in such cases are yet to be properly addressed: Though the analytic method can, in principle, be extended to general pupils, as pixelated pupil shape becomes more complex, analytic calculations can be challenging; Any pupil shape change can compound complexity and inefficiency in executing the method in real-time, due to constructing the analytic forms of orthonormal polynomials whenever pupil shape changes.

Previously, three ways of computing orthonormal aberration polynomials and their coefficients are discussed. The methods use the Gram-Schmidt (GS) process but differ in the way of computing key integrals during the GS process. The first method analytically computes the integrals, where a computer algebra program is used. The second uses the Gaussian quadrature over triangulated pupil geometry. The last uses indirect estimates of the integrals, which turned out to be natural by-products of the usual least-square Zernike polynomials fit. It is shown that the first method would be limited to simple pupil geometry, while the second can be applied to more general pupil shapes. However, when dealing with complicated variable non-circular pupils, the last method can be vastly more efficient than the second and enables the possibility of estimating orthonormal aberration coefficient on the fly. Also noticed is that the last method naturally takes into account the pixilation effect of pupil geometries due to pixel-based imaging sensors (e.g. CCDs). With these benefits, the last method can be used as a viable tool in real-time wavefront analysis over dynamically changing pupils and has been implemented for the HET Wavefront sensors, which turned out to be quite efficient and stable based on the on-sky data presented in the subsequent sections.

2. THEORY

The Zernike polynomials (Zi) can be identified by radial and angular orders [n,m][11]. The polynomial index scheme used here follows: Zi[n1,m1] precedes Zj[n2,m2] if n1 < n2; if n1 = n2 and |m1| < |m2|, Zi precedes Zj ; if n1 = n2, |m1| = |m2|, and m1 < 0, Zi precedes Zj . Suppose a wavefront function W(x, y) on a non-circular pupil E that is a subset of a unit disk S. Assume that W can be described in terms of M Zernike polynomials.

$$W = \alpha_1 Z_1 + \alpha_2 Z_2 + \cdots + \alpha_M Z_M = \vec{\alpha}^T \vec{Z} \tag{1}$$

where $\vec{\alpha}$ and $\vec{Z}$ are the column vectors of α_i and Z_i respectively, and T means transpose. The estimation of αi can be written with A being the area of E as,

$$\sum_{j=1}^{M} \alpha_j F_{ij} = \sum_{j=1}^{M} \alpha_j \iint_E \frac{Z_i Z_j}{A} dA = \iint_E \frac{Z_i W}{A} dA \tag{2}$$

Z_i are not orthonormal over E and thus a M x M matrix F, whose (i, j) element is F_{ij}, is neither unitary nor diagonal. The estimate of α_i can still be given by,

$$\boxed{\alpha_{i,e} = \sum_{j=1}^{M} G_{ij} \iint_E \frac{Z_i W}{A} dA} \tag{3}$$

with G_{ij} being the (i,j) element of $\iint \frac{Z_i Z_j}{A}$. $\alpha_{i,e}$ is neither α_i nor the desired orthonormal aberration coefficient (β_i) of W on E, but closely related to β_i as follows. It is widely known that new orthonormal polynomials, say U_i, can be determined by the Gram-Schmidt orthonormalization of a known set of orthonormal polynomials (Z_i in our case) [12]. Letting $U_1 = Z_1$, we have

$$V_j = Z_j - \sum_{k=1}^{j-1} C_{jk} U_k, \qquad U_j = V_j \sqrt{A / \iint_E V_j V_j \mathrm{dA}}, \tag{4}$$

where j = 1, 2, …, M. Using Eq. 4, the following algebraic relation is obtained.

$$\iint_E \frac{V_i V_j}{A} \mathrm{dA} = F_{ij} + \sum_{m=1}^{i-1} \left\{ \sum_{n=1}^{j-1} C_{im} \delta_{mn} C_{nj} \right\} - \sum_{n=1}^{i-1} C_{in} C_{nj} - \sum_{m=1}^{j-1} C_{im} C_{mj}, \tag{5}$$

with δ_{mn} being the Kronecker delta. Given the orthogonality of V_i, the left-hand size of Eq. 5 equals to C_{ii} for $i = j$ or vanishes for $i \neq j$. This reduces Eq. 5 to the following algebraic expressions of the Gram-Schmidt orthonormalization coefficient C_{ij}.

$$C_{ii} = \sqrt{F_{ii} - \sum_{k=1}^{i-1} C_{ik}^2}\,, \quad C_{ij} = \frac{F_{ij}}{C_{jj}} - \sum_{k=1}^{j-1} \frac{C_{ik} C_{jk}}{C_{jj}} \tag{6}$$

$C_{i,j}$ is essentially the (i,j) element of a M x M lower triangle matrix **C** which can be obtained from the Cholesky decomposition of F as noted in a different way elsewhere [9]. From Eq. 4, we obviously obtain

$$\vec{Z} = \mathbf{C}\vec{U} \quad \text{and} \quad \vec{U} = \mathbf{D}\vec{Z} \tag{7}$$

where **D** is $\mathbf{C}^{-1}$. Multiplying $\vec{\alpha}_e$ (the vector of $\alpha_{i,e}$) to Eq. 7 yields a relation between $\vec{\alpha}_e$ and $\vec{\beta}$, also recognized in [9], as,

$$\boxed{\overrightarrow{\alpha_e}^T \mathbf{C} = \vec{\beta}^T \quad \text{and} \quad \vec{\beta}^T \mathbf{C}^{-1} = \vec{\beta}^T \mathbf{D} = \vec{\alpha}_e^T} \tag{8}$$

The above orthonormalization process clearly indicates that knowing **F** is central to computing **C** and constructing analytic forms of U which can be fitted to wavefront data to determine $\vec{\beta}$. This analytic derivation of **F** can be done for simple pupil shapes, but it can be non-trivial over a complicated pupil domain even using a computer algebra software [13].

3. IMPLEMENTATION

The above process of constructing the orthonormal polynomials over an arbitrary geometry can be numerically implemented via Cholesky decomposition of the Zernike Norm matrix, results in a conversion matrix C, that can be used to convert the Zernike matrix into orthonormal matrix over the given pupil domain E or to transform the sub-optimal Zernike coefficients into the optimal orthonormal coefficients over E [14]. Likewise, the alignment sensitivity matrix defined as Zernike coefficients can also be converted into a new sensitivity matrix based on the optimal coefficients, hence the alignment offsets can be uniquely estimated regardless of the telescope pupil shape. All of these procedures are written in C++ WFS library at the HET.

Since the HET pupil contains a number of non-trivial obscuration geometries, it was necessary to measure their shapes, orientations, and motion coefficients at different HET tracker positions in order to build the HET pupil model. As part of the HET Wide-Field Upgrade, we built a Pupil Viewing Camera (PV) into the telescope metrology system. Using the PV at different tracker positions, we recorded the pupil obscuration geometries and constructed the HET pupil model that describes the location and orientation of these geometries as functions of the tracker coordinates as shown in Figure 2. Left two columns in the figure shows the HET pupil as seen by the PV at various tracker positions. The top in the last column is the HET pupil model at an arbitrary tracker position. The bottom in the same column shows the image from one of two HET WFS with the HET pupil geometries as well as the WFS sub-aperture geometry overlaid.

During the observing track, the HET Telescope Control System (TCS) transmits the HET tracker 6DOF coordinates (x, y, z, clocking, tip, tilt) into the subsystem called the Payload Alignment System (PAS). The PAS is then parse the information into the WFS pipeline. The tracker coordinate information is used to set the tracker-dependent pupil geometries such as the segmented primary mirror and the tracker bridge structure. The PAS also transmits the coordinates of the WFS probe on the focal surface of the telescope. This coordinate defines the field position of the probe and is used to set the field-dependent pupil geometries such as some of the obscurations caused by the internal optics of the wide-field corrector.

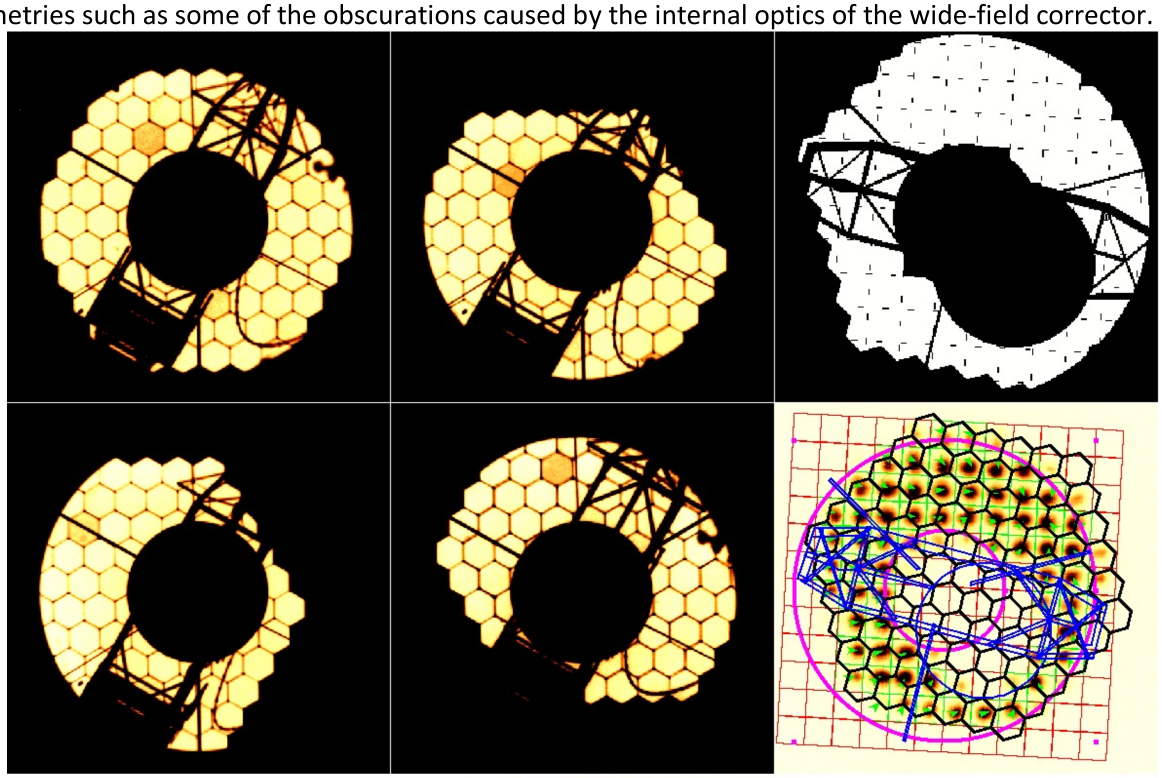

Figure 2 . (Left two columns) Pupil geometries measured at various tracker locations by the HET pupil viewing camera. (Right column) Numerically constructed pupil domain at a given track position (top) and the geometries imposed on the HET WFS image frame (bottom).

4. ON-SKY PERFORMANCE

Over the past few years, the individual HET metrology instruments have been constructed and tested in Austin lab and on-sky commissioned in 2016 and early part of 2017. The HET metrology instruments include two WFS, two Guide Probes (GP), a Tip/Tilt camera (TTCam), and a Distance Measuring Interferometer (DMI). The WFS and GP are the ones that measure the telescope pointing and alignment through the entire optical chain of the telescope. Their update rates are 15sec and 5sec, respectively. The TTCam and DMI measure the telescope's mechanical alignment at much higher frame rates. Together, these instruments provide redundant information on the telescope alignment.

The software effort has been the major item since then in order to fine tune the loop behavior of alignment control of the telescope using all information coming from these metrology instruments. The main alignment feedback comes from two WFS. These feedbacks are used within the TCS to guide the telescope alignment through a PID control loop. Since the update rate of the WFS is slower than TTCam and DMI, its alignment offset information is instead used to update the offset fiducial points for the DMI and TTCam, to which these instruments drive the telescope alignment.

One example of this combined control loop is shown in Figure 3. The WFS offset measured across little less than 2hr-long track shows well maintained focus (±25μm) and tip/tilt (±5 arcsec) alignment of the telescope. Also shown is the guider image quality that remains under 1.4 arcsec in FWHM over the entire track. The median image quality of the HET at the guider field (11 arcmin radial field) is 1.4 arcsec. Over this track, the HET pupil went through a substantial variation. Despite this, the numerical orthonormalization process in the WFS pipeline stabilized the aberration estimation process, that resulted in consistent telescope alignment offsets. Another WFS active alignment performance is shown in Figure 4 on a different night with similar behavior. Hence the suite of metrology instruments and their control loop are effectively keeping the telescope in alignment.

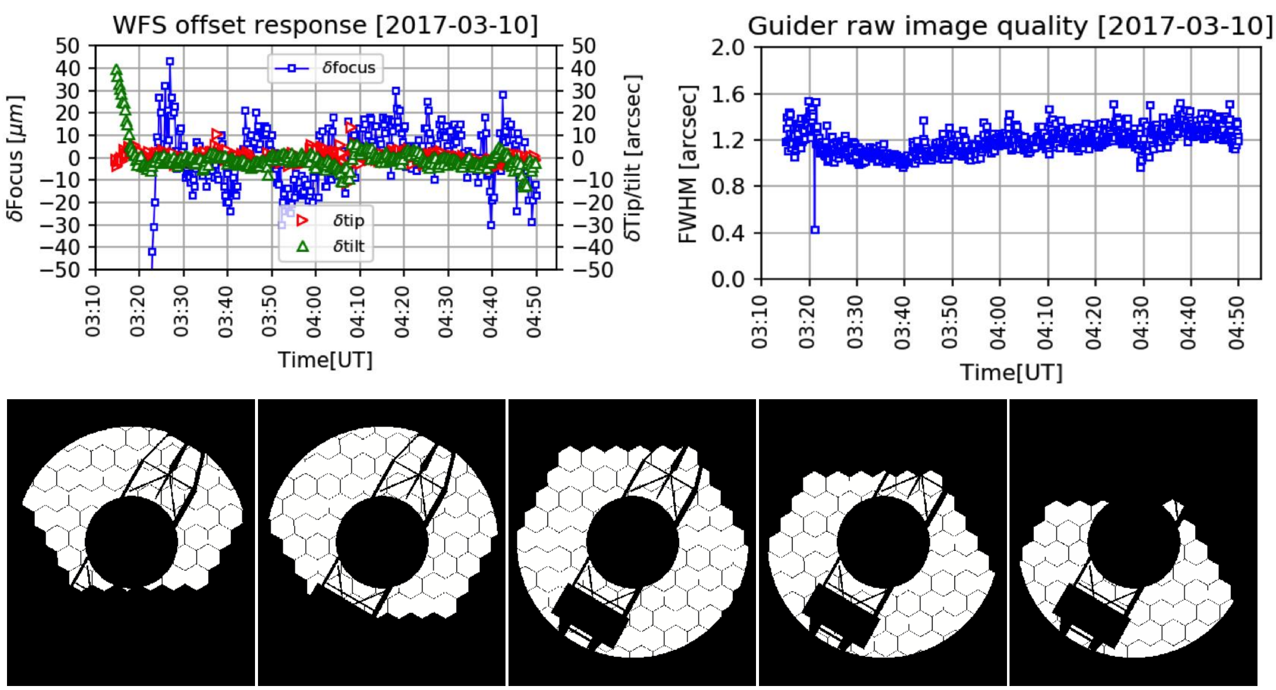

Figure 3 Example closed loop active alignment performance of the HET WFS on 2017-3-10 (Top Left) and the guider image quality in the full-width at half-max (FWHM) (Top Right). The HET pupil model over the track (Bottom)

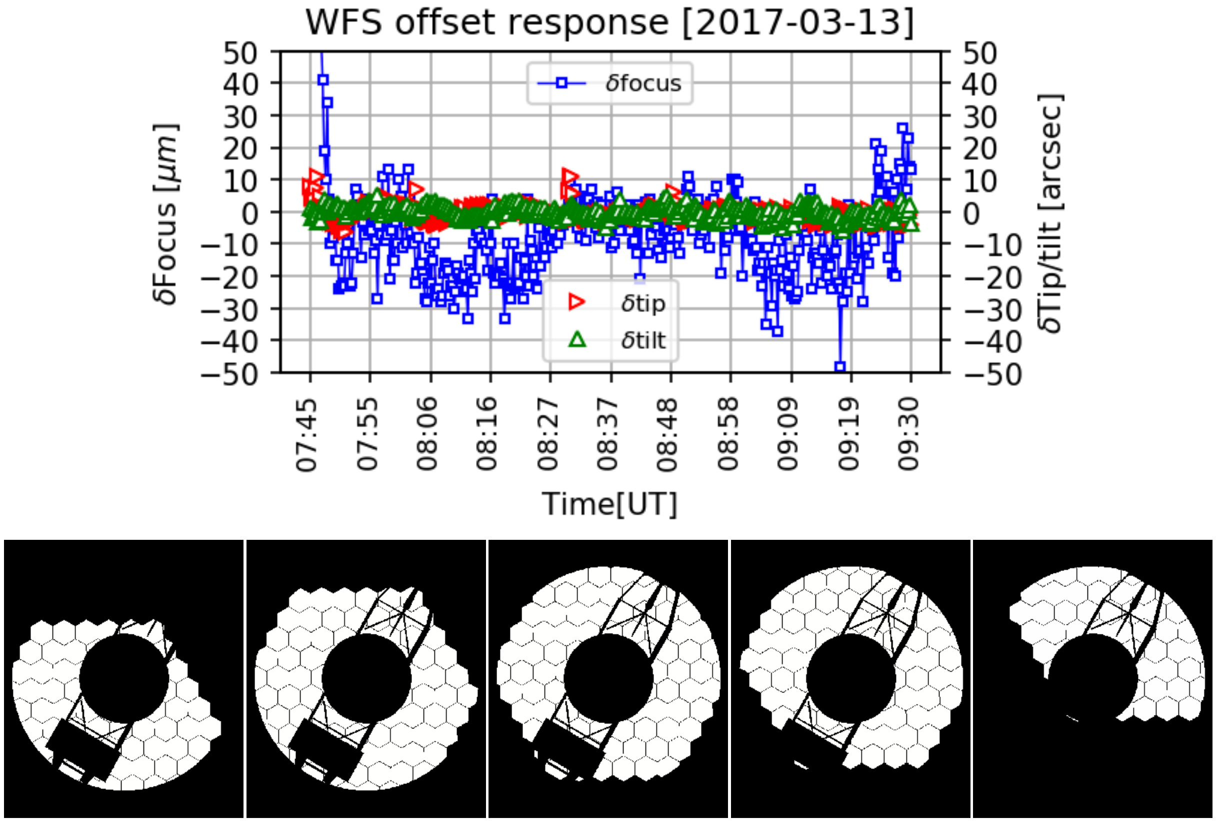

Figure 4 Another example of the closed loop active alignment performance of the HET WFS on 2017-3-13 (Top) and the corresponding HET pupil model (Bottom).

5. CONCLUSION

In this paper, we discussed the application of numerical orthonormalization of aberration functions to telescope systems with dynamically varying non-circularly symmetric pupil shapes. The unique situation arises when implementing wavefront sensing on such telescope systems as the telescope pupil is no long circularly symmetric and the usual aberration functions become non-orthonormal and the resultant aberration coefficients are not unique. Any physical parameters derived from these non-unique aberration coefficients are non-unique as well. Therefore, this poses a challenge in active alignment control of the prime focus camera using Shack-Hartmann wavefront sensing feedback. As presented, we developed a method to construct orthonormal modal functions as the telescope changes in pupil geometry and to make the alignment offsets, derived from the low-order aberration modes, robust against such a variation. We implemented this method in the HET TCS and commissioned this method in the metrology system of the Hobby-Eberly Telescope over the last year and a half. We also highlighted some of the on-sky data from the WFS active alignment loop. These on-sky data showed that the implemented numerical orthonormalization technique indeed stabilized the WFS over dynamically varying telescope pupil geometries and maintained the image quality of the telescope over 22 arcmin field of view over 2hr long observing tracks.

ACKNOWLEDGEMENTS

HETDEX is led by the University of Texas at Austin McDonald Observatory and Department of Astronomy with participation from the Universitäts-Sternwarte of the Ludwig-Maximilians-Universität München, the Max-Planck-Institut für Extraterrestriche-Physik (MPE), Astrophysikalisches Institut Potsdam (AIP), Texas A&M University, Pennsylvania State University, and the HET consortium. In addition to Institutional support, HETDEX is funded in part by gifts from Harold C. Simmons, Robert and Annie Graham, The Cynthia and George Mitchell Foundation, Louis and Julia Beecherl, Jim and Charlotte Finley, Bill and Bettye Nowlin, Robert and Fallon Vaughn, Eric Stumberg, and many others, by AFRL under agreement number FA9451-04-2-0355, and by the Texas Norman Hackerman Advanced Research Program under grants 003658-0005-2006 and 003658-0295-2007.

REFERENCES

[1] G. Hill, et al., “Completion and performance of the Hobby-Eberly telescope wide field upgrade,” Proc. SPIE, **10700-20** (2018).

[2] H. Lee, et al., “Analysis of active alignment control of the Hobby-Eberly Telescope wide field corrector using Shack-Hartmann wavefront sensors,” Proc. SPIE, **7738**-18 (2010).

[3] H. Lee, et al., “New Hobby Eberly telescope metrology systems: design, implementation, and on-sky performance,” Proc. SPIE, **10700-78** (2018).

[4] F. Zernike, “Diffraction theory of knife-edge test and its improved form, the phase contrast method," Mon. Not. R. Astron. Soc. **94,** 377 (1934).

[5] N. Roddier, “Atmospheric wavefront simulation using Zernike polynomials," Opt. Eng. **29**, 1174 (1990).

[6] H. Lee, G. B. Dalton, I. A. Tosh, S.-W. Kim, ”Computer-guided alignment I : Phase and amplitude modulation of alignment-influenced optical wavefront," Optics Express **15,** 3127 (2007).

[7] C. F. Dunkl, SIAM J., “Orthogonal polynomials on the hexagon,'' SIAM J. Appl. Math.**47**, 343 (1987).

[8] R. Upton and B. Ellerbroek, “Gram-Schmidt orthogonalization of the Zernike polynomials on apertures of arbitrary shape,'' Optics Letters **29**, 2840 (2004).

[9] G. Dai and V. Mahajan, “Nonrecursive determination of orthonormal polynomials with matrix formulation,” Optics Letters **32**, 74-76 (2007).

[10] V. N. Mahajan and G. Dai, “Orthonormal polynomials in wavefront analysis: analytical solution,” Journal of Optical Society of America A. **24**, 2994 (2007).

[11] M. Born and E. Wolf, Principles of Optics, 7th ed. (Oxford, 1999).

[12] G. B. Arfken, H. J. Weber, F. Harris, Mathematical Methods for Physicists, 5th ed. (Academic,2001).

[13] Maxima ver. 5.18.1 (A Computer Algebra System), http://maxima.sourceforge.net/

[14] H. Lee, “Use of Zernike polynomials for efficient estimation of orthonormal aberration coefficients over variable non-circular pupils,” Optics Letters Vol. 35, 2173-2175 (2010).